

## Charge fluctuations between CuO<sub>2</sub> layers in high-temperature superconductors

R. Friedberg and T. D. Lee

Columbia University, New York, New York 10027

(Received 23 January 1989)

A simple model based on the phase transition between a Bose liquid and a Fermi gas is presented. We show that under certain assumptions the long-range (distance greater than 3 Å) Coulomb forces favor charge fluctuations between neighboring CuO<sub>2</sub> layers in high-temperature superconductors, provided that the number  $n$  of CuO<sub>2</sub> layers within a unit cell is 2 or greater (with the convention that  $n=1$  for La 2:1:4 and  $n=2$  for Y 1:2:3, etc.). Qualitative discussion of the variation of  $T_c$  on  $n$ , and on the doping parameter, is given.

### I. GENERAL DISCUSSION

#### A. Boson dissociation and energy gap

One of the striking features<sup>1,2</sup> of the high-temperature superconductors is the smallness of the "coherent length"  $\xi \approx 10$  Å, which is much less than the normal type-1 or type-2 superconductors. The parameter  $\xi$  measures the radius of the magnetic filament that penetrates the superconductor, whose flux is quantized in units of  $2\pi\hbar c/2e$ . This indicates a pairing mechanism between electrons or holes that is reasonably well defined in the coordinate space. Therefore, one may represent the pair state by a phenomenological local boson field  $\phi(\mathbf{r})$  whose mass  $m$  is  $\approx 2m_e$ , and its elementary charge unit is  $\pm 2e$ , where  $m_e$  and  $e$  are the mass and (the magnitude of) charge of an electron. The gap energy  $\Delta$  has been observed,<sup>1,3</sup> and is of the order

$$\Delta \sim kT_c, \quad (1.1)$$

where  $T_c$  is the critical temperature and  $k$  the Boltzmann constant. The apparent localization of the pairing makes it natural to explore the analogy<sup>4,5</sup> with liquid helium (at least as an alternative theoretical possibility, different from the conventional BCS approach). However, there are two major differences.

(i) Helium is electrically neutral, while a superconductor must have charged particles. One of the main concerns of this paper is to examine the effects of the long-range Coulomb forces of these charged particles.

(ii) The  $\Lambda$  transition of He is determined by the Bose-Einstein transition, where the critical temperature  $T_B$  is given by

$$\lambda_T \equiv (2\pi\hbar^2/mkT_B)^{1/2} \sim \rho^{-1/3} \quad (1.2)$$

with  $\lambda_T$  as the thermal wavelength and  $\rho$  as the number density. For He,  $T_B$  is 2.2 K. If one applies (1.2) to the new high-temperature superconductors, then for  $m \approx 2m_e$ ,

$$T_B \sim (\rho/\rho_{\text{He}})^{2/3} (m_{\text{He}}/m) \times 2.2 \text{ K} \approx 2000 \text{ K}. \quad (1.3)$$

Alternatively, one may set  $T_B = T_C \sim 10^2$  K, then  $m$  would be about  $40m_e$ , which also seems to be unusually large. [For bosons with an anisotropic inertia tensor of

eigenvalues  $m_x$ ,  $m_y$ , and  $m_z$ ; the  $m$  in (1.2) and (1.3) is  $(m_x m_y m_z)^{1/3}$  which, for  $m_x = m_y = 2m_e$ , would require  $m_z = 1.6 \times 10^4 m_e$  to have  $m = 40m_e$ .]

This difficulty may be circumvented by assuming the individual quantum (i.e., the pair state) of the phenomenological boson field  $\phi$  to be unstable with

$$\phi \rightarrow 2 \text{ holes (or } 2e). \quad (1.4)$$

We represent the condensate by a Bose liquid, made of a macroscopic number of  $\phi$  quanta. Let  $\Delta$  be the binding energy per  $\phi$  quanta in the liquid phase, and  $m - 2m_e$  be the mass difference in (1.4). Under the assumption

$$\Delta > (m - 2m_e)c^2 > 0 \quad (1.5)$$

(with  $c$  = velocity of light), the macroscopic system can be in either a Bose-liquid phase, or a Fermi-gas phase; the latter is very different from liquid He I. The order of magnitude of the critical temperature is then given by (1.1), not (1.2). Thereby, the difficulty of (1.3) is avoided.

#### B. Bose-liquid and Fermi-gas model

At low temperature, the system is in the Bose-liquid state, which is a three-dimensional superfluid (such as liquid He II). At high temperature, it is in a Fermi-gas state; hence, the usual band theory of normal electrons (or holes) in a conductor becomes applicable.

To overcome certain habitual associations with respect to liquid helium which would be misleading here, we offer the following mutilation of helium physics to make the analogy closer. Imagine that the helium nucleus were unstable to fission into deuterium. But suppose the energy of dissociation were less than the binding energy per atom of liquid He II. Then at absolute zero temperature He II would be the favored state, but as the temperature was raised in a container of fixed volume, He II would coexist with deuterium gas in diminishing ratio until all the liquid He would evaporate at some temperature  $T(\rho)$  that depends on the total amount in the container, but which we take to be *much less than* 2.2 K. This could be achieved in our hypothetical case by near equality of the dissociation energy  $\text{He} \rightarrow 2\text{D}$  and the binding energy of the liquid.

In such a world, *neither He gas nor liquid He I would exist*. Helium would form only at microtemperatures from deuterium gas by direct condensation into liquid He II. It is this process that we propose as analog to the high-temperature superconducting transition in ceramics. (Here, the term "ceramics" is used even though its normal state is a conductor.)

In this analogy, an electron hole corresponds to an atom of deuterium. Since the composition of the ceramic determines the overall density of holes, the process of heating the superconducting ceramic is indeed like that of heating a liquid-gas mixture in a closed container. This differs in two important ways from the usual process of heating a liquid at fixed pressure.

First, in closed-container heating one does not arrive at the critical point, unless the fixed overall density was properly chosen to be the critical density  $\rho_c$ . For orientation purposes, assume that if the "liquid-gas" system in ceramic superconductors has a critical point, the critical density is greater than the hole density achievable in practice. In heating at fixed subcritical density, the liquid will gradually evaporate and one is left with pure vapor at a temperature less than critical.

Thus, the temperature  $T(\rho)$  at which all the liquid disappears, which is customarily called  $T_c$  for the superconductor, does *not* correspond to the liquid-gas critical temperature; the latter only pertains to one special  $\rho = \rho_c$ . Rather,  $T(\rho)$  is that temperature for which the gas at coexistence attains the given density  $\rho$ .

Second, away from the true critical point the liquid-gas transition is first order. Yet in closed-container heating one does not observe the expected discontinuities, for example, in the total energy. These discontinuities exist between the two phases, but the system does not convert in bulk at a sharp temperature from one phase to the other. In other words, a confined liquid does not boil if heated slowly. The pressure of the gas simply mounts along with the vapor pressure of the liquid, until all the material has smoothly evaporated.

Therefore, following this analog, we may speak of the superconducting transition in ceramics as first order,<sup>6,7</sup> even though no latent heat is observed because calorimetry does not distinguish the two coexisting phases.

At zero temperature, the system is in the Bose-liquid phase. As temperature rises, the evaporation into the Fermi-gas phase forms a Fermi sea with a top kinetic energy which may be much greater than the energy gap  $\Delta$ . In Appendix A we discuss why such a Fermi sea does not prohibit the continuing evaporation process with increasing temperature.

One naturally pictures the coexisting liquid and gas as occupying separate volumes. But there is another option: In our hypothetical world, deuterium might exist as a solute gas inside the liquid He II. This would explain the same phenomena, unless one looked inside the container to see whether the two phases were separated.

### C. Separation of phase and Coulomb energy

In ceramic superconductors, each boson or fermion carries an electric charge  $2e$  or  $e$ . The *overall* density is just

enough to balance the net negative density of fixed background charge. Therefore, it would seem impossible to have two separate phases of different density, as neither phase would be electrically balanced and the Coulomb energy would be huge. By this reasoning, the Fermi gas must be "dissolved" in the Bose liquid.

There is, however, a compromise option. Fermi gas and Bose liquid might separate onto adjacent layers of  $\text{CuO}_2$ . They would then screen one another about as effectively as the net positive charge on the  $\text{CuO}_2$  is screened by negative charges on the other layers.

The main purpose of our paper is to explore this latter option in relation to the number and spacing of  $\text{CuO}_2$  layers. To this end, we separate the energy of the bosons into a long-range Coulomb part, for which we can make detailed calculations depending on the layer spacing, and a short-range phenomenological part, whose form we can only guess but which we assume to be unaffected by anything outside a given  $\text{CuO}_2$  layer except its nearest-neighbor atoms (see Sec. ID).

Our calculations in this paper will be restricted to zero temperature, at which the Fermi gas is infinitely dilute. Hence, "separation" simply means that the Bose liquid occupies some layers and not others. We shall also use the term "charge fluctuation" to denote this situation.

Phenomenologically, one may separate the interaction energy  $U$  into a short-range  $U_\phi$  and a long-range Coulomb term  $U_c$ :

$$U = U_\phi + U_c, \quad (1.6)$$

where  $U_\phi$  can be written as

$$U_\phi = \int u(\rho) d^3r \quad (1.7)$$

with  $u$  as a local function of the charged boson-density

$$\rho \equiv \phi^\dagger \phi. \quad (1.8)$$

In a typical high- $T_c$  superconductor, the crystal structure is orthorhombic with the lengths of the two short axes  $a$  and  $b$  in the neighborhood of 3.8 Å; the long axis  $c$  is approximately given by

$$c = (n-1)c_1 + c_2, \quad (1.9)$$

where  $n$  is the number of  $\text{CuO}_2$  planes per unit cell,  $c_1$  is typically  $\sim 3.2$ – $3.3$  Å, and  $c_2$  varies from 6.59 Å in La 2:1:4 to 11.54 Å in Tl 2:2:2:3. The distance between nearest-neighboring Cu and O sites is  $\frac{1}{2}a \approx \frac{1}{2}b$  and that between neighboring O sites is  $a/\sqrt{2}$ . Both are smaller than 3 Å. We assume that the pairing and the phenomenological local interaction function  $u(\rho)$  are due mainly to all forces (Coulomb, spin-spin, and exchange) at these small distances  $< d$  ( $\approx a = b \approx 3.8$  Å) in the same  $\text{CuO}_2$  plane. The long-range Coulomb term  $U_c$  in (1.6) includes all electrostatic forces between charged particles on different  $\text{CuO}_2$  planes (spacing at  $c_1$  or  $c_2$  from each other), as well as between those on the same  $\text{CuO}_2$  plane that are at distances  $\geq d$  from each other.

Of course, there is some arbitrariness in the value  $d$ . But since  $U_\phi$  by its form is insensitive to density fluctuations in lengths  $< d$ , we want  $d$  as small as possible provided that  $U_\phi$  includes all non-Coulomb effects. This

gives, as a lower bound  $d = a$  or  $b$ .

The Bose liquid is composed of the  $\phi$  quantum. Each  $\phi$  quantum is essentially two dimensional, with a linear size of the same order as  $d$ , and these quanta hop from lattice site to lattice site (in the three-dimensional space). Since, as will be discussed in Sec. ID, each boson involves two  $O^-$  ions, we associate the bosons with their center-of-mass positions, the  $Cu^{2+}$  sites. Let  $Q_i$  be the charge-density operator of the  $\phi$  field at the  $i$ th lattice site. The purely bosonic part of the long-range Coulomb interaction can be written as

$$(U_c)_{\text{boson}} \cong \frac{1}{2} \sum_{i \neq j} Q_i Q_j / r_{ij}. \quad (1.10)$$

The restriction  $i \neq j$  is equivalent to assuming that

$$d = a \text{ or } b. \quad (1.11)$$

As we shall see, a larger  $d$  means more charge fluctuation for the Bose liquid; therefore (1.11) also serves as a lower bound for the estimation of charge fluctuation. Coulomb interactions in the same  $CuO_2$  plane, but over distances  $< d$ , are excluded here, since they are already included in  $U_\phi$ . In the Fermi-gas phase, we have the standard conduction electrons, whose density may be approximated by a uniform one. The decomposition (1.6) of the interaction energy  $U$  applies only when the system is either in a pure Bose-liquid phase, or in the two-phase region.

In Fig. 1, we give an example of the local energy density function  $u(\rho)$  that appears in (1.7). Because of the instability (1.4) and the inequality (1.5),

$$u(\rho) \rightarrow (m - 2m_e)c^2\rho \text{ as } \rho \rightarrow 0, \quad (1.12)$$

and in order to have  $\Delta > 0$ ,  $u(\rho)$  must be negative (attractive) at some range of  $\rho$ . Let  $\overline{OL}$  be tangent to  $u(\rho)$  with  $O$  denoting the origin ( $\rho = 0$ ) and  $L$  the tangent point on  $u(\rho)$ . If there were no long-range Coulomb interaction (i.e., if  $U_c = 0$ ), then at any density  $\rho < \rho_L$ , the density at  $L$ , the system would separate into two phases: At zero temperature the system condenses into a Bose liquid which occupies only a fraction  $\rho/\rho_L$  of the total volume  $\Omega$ . This can be readily seen by considering any point  $P(\rho_P, u_P)$  on the line segment  $\overline{OL}$ , and noting that, as shown in Fig. 1,

$$u(\rho_P) > u_P = u_L \rho_P / \rho_L, \quad (1.13)$$

where  $u_L = u(\rho_L) = -\Delta$ , the negative of the binding ener-

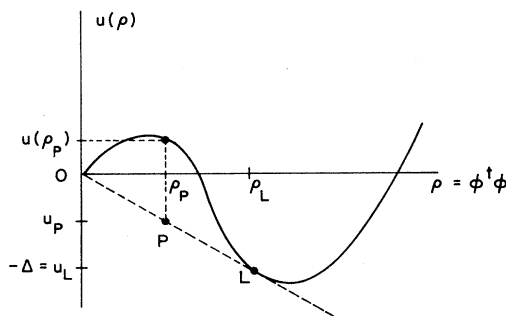


FIG. 1. A schematic drawing of the local energy density  $u(\rho)$  vs the boson density  $\rho$ .

gy per boson. Thus, if  $U_c$  were zero, the liquid in the two-phase region is represented by  $L$ . On the other hand, since  $U_c \neq 0$ , such a large-scale density fluctuation between the liquid and the gas also means a large charge fluctuation. Of course, to minimize the Coulomb energy, each unit cell would be electrically neutral. But within a cell, there could still be charge fluctuation between neighboring  $CuO_2$  planes.

Other things being equal, one might first suppose that the Coulomb energy would be minimized by distributing charge evenly between two equivalent layers, and therefore that the separation of phases in layers would take place only if the inequality (1.13) were stronger than the Coulomb effect. Actually, we find that the Coulomb effect may possibly favor separation. As we shall see, the answer depends sensitively on the number of  $CuO_2$  layers per cell and the ratios between lattice spacings  $a$ ,  $b$ ,  $c_1$ , and  $c_2$ .

Consider two  $CuO_2$  planes at a spacing  $c_1 \cong 3.2 \text{ \AA}$  from each other. The Coulomb energy of two neighboring  $\phi$  quanta on different  $CuO_2$  planes can be as large as  $(2e)^2/c_1$ . However, if these two  $\phi$  quanta are placed on the same  $CuO_2$  plane, their contribution to  $U_c$  would be  $\leq (2e)^2/d$ . Because  $d \cong a > c_1$ , the latter energy can be smaller than the former. In this picture, the long-range Coulomb interaction  $U_c$  would favor charge fluctuations between neighboring  $CuO_2$  planes.

It may be objected that if two quanta are on closely neighboring planes they will simply avoid each other so as not to incur the maximum energy  $(2e)^2/c_1$ . But doing so will cost a kinetic energy that may well be of the same order. The (superfluid) Bose liquid must contain a substantial zero-momentum component, which acts against such an increase of kinetic energy. For simplicity, we assume that kinetic "stiffness" dominates so that in evaluating  $U_c$  the charge distribution within each plane is uncorrelated with the other. But any cost of exclusion of two quanta on the same plane from a single site is already part of  $U_\phi$ .

The detailed calculation of charge fluctuation will be given in Secs. II and III. For simplicity, take the temperature to be zero. Hence, we have only the Bose liquid. Its charge fluctuation produces a long-range Coulomb energy, since there is no Fermi gas (normal conduction electrons) to screen the effect; the polarization due to other material present only reduces the Coulomb potential by a factor  $\epsilon$ , where  $\epsilon$  is the dielectric constant. As we shall see, in La 2:1:4 ( $n=1$ ) the long-range Coulomb force is against any charge fluctuation. Hence, the dependence of  $\Delta$  on the doping parameter  $y$  reflects directly the function  $u(\rho)$ . On the other hand, in Y 1:2:3 ( $n=2$ ) large charge fluctuations can occur between neighboring  $CuO_2$  planes within the same unit cell. The dependence of  $\Delta$  on the doping parameter  $x$  is then a convolution function of  $u(\rho)$ ; the result is for  $\Delta$  to acquire a "steplike" variation versus  $x$ . A similar feature should also manifest itself in  $T_c$  vs  $x$ .

#### D. An example of pairing mechanism

The long-range Coulomb interaction is not sensitive to the details of the pairing mechanism nor the the underlying

ing basis of the local energy density  $u(\rho)$ . Yet, for applications to superconductors such as

$$(\text{La}_{1-y}\text{Sr}_y)_2\text{CuO}_4 \text{ and } \text{YBa}_2\text{Cu}_3\text{O}_{6.5+x}, \quad (1.14)$$

a concrete model might be useful; it would help one, among other things, to relate the boson density  $\rho$  to the doping parameters  $x$  and  $y$ . In the following, we give a highly simplified model<sup>6</sup> in which the pairing mechanism is an adaptation of the ideas of Aharony *et al.*,<sup>8</sup> Birgeneau, Kastner, and Aharony,<sup>9</sup> and Uemura.<sup>10</sup> This model is not a necessary premise for the calculations to follow, but it may render our ideas about the function  $u(\rho)$  plausible.

It is well known that, e.g., La 2:1:4 is antiferromagnetic when  $y=0$ . Superconductivity<sup>11,12</sup> appears when  $y$  is approximately greater than or equal to 0.025, and it disappears when  $y$  is  $\sim 0.15$ . Because  $\text{La}=\text{La}^{3+}$ ,  $\text{Sr}=\text{Sr}^{2+}$ ,  $\text{Ba}=\text{Ba}^{2+}$ , and  $\text{Cu}=\text{Cu}^{2+}$ , when  $y=0$ , all O are  $\text{O}^{2-}$ . When  $y$  is greater than 0, some  $\text{O}^{2-}$  turn into  $\text{O}^-$ . Phenomenologically, one may give the interpretation  $\text{O}^{2-}$  creates antiferromagnetism in the  $\text{Cu}^{2+}$  spins on a  $\text{CuO}_2$  plane, while  $\text{O}^-$  destroys antiferromagnetism and induces superconductivity. Likewise, in Y 1:2:3, when  $x=0^-$  we have  $\text{Y}=\text{Y}^{3+}$ ,  $\text{Ba}=\text{Ba}^{2+}$ ,  $\text{Cu}=\text{Cu}^{2+}$ ,  $\text{O}=\text{O}^{2-}$ , and the substance is antiferromagnetic. Superconductivity<sup>13-15</sup> arises only for  $x > 0$  when some O become  $\text{O}^-$ .

Take the covalent-bond picture. In a linear  $\text{Cu}^{2+}-\text{O}^--\text{Cu}^{2+}$  chain, the extra ( $2p$ ) electron in  $\text{O}^-$  likes to spread out its wave function toward both  $\text{Cu}^{2+}$  in order to decrease its kinetic energy (and also increase the Coulomb attraction). This is possible if its spin is antiparallel to the hole spin in each  $\text{Cu}^{2+}$  ( $3d^9$ ), making the two  $\text{Cu}^{2+}$  spins parallel. On the other hand, in a  $\text{Cu}^{2+}-\text{O}^{2-}-\text{Cu}^{2+}$  chain, since the spins of the two extra  $e^-$  in  $\text{O}^{2-}$  are antiparallel, each of which is, in turn, antiparallel to the hole spin of one of the neighboring  $\text{Cu}^{2+}$ , the two  $\text{Cu}^{2+}$  spins are also antiparallel. Because the latter is through a high-order (superexchange<sup>16</sup>) process, its energy preferential  $\epsilon_{\uparrow\downarrow}$  is much smaller than the former  $\epsilon_{\uparrow\uparrow}$ . In the  $\text{CuO}_2$  plane of, say,  $\text{YBa}_2\text{Cu}_3\text{O}_{6.5+x}$ , when  $x=0^-$  all neighboring Cu spins are antiparallel; the system is therefore antiferromagnetic. When  $x > 0$ , the appearance of  $\text{O}^-$  destroys the antiferromagnetism. From Figs. 2(a) and 2(b), we see that an isolated  $\text{O}^-$  forces three pairs of Cu spins in the  $\text{Cu}^{2+}-\text{O}^{2-}-\text{Cu}^{2+}$  bond to be parallel (called "frustrated" bond), whereas a pairing of two  $\text{O}^-$  produces only two frustrated bonds,<sup>8-10</sup> instead of six frustrated bonds if unpaired. Thus, there is a tendency to pair  $\text{O}^-$ . Each  $\text{O}^-$  (being  $2p^5$ ) carries a hole; the Bloch wave of the oxygen-hole pair can then be represented by a boson field  $\phi$ . When all  $\text{O}^-$  are paired to form  $\phi$  on the  $\text{CuO}_2$  planes, we have the (maximum) boson density

$$\rho = \frac{1}{2} x = y \text{ per } \text{CuO}_2 \text{ layer per cell.} \quad (1.15)$$

As shown in Figs. 2(c) and 2(d), there is also the possibility of the clustering of four  $\text{O}^-$  or six  $\text{O}^-$ , each of which carries no frustrated bond, thus further decreasing the magnetic energy (though increasing the Coulomb energy). We hypothesize that the gain in the antiferromagnetic energy  $\epsilon_{\uparrow\downarrow}$  overcomes the Coulomb repulsion. (This requires the short-range Coulomb energy to have a large

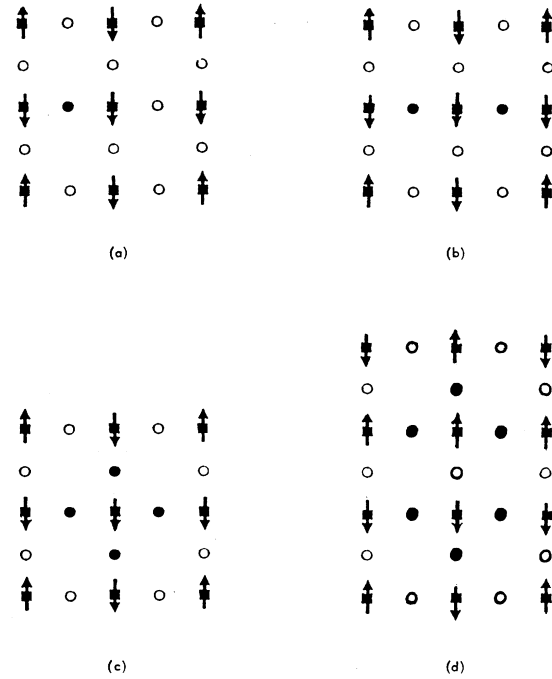


FIG. 2. Filled squares are  $\text{Cu}^{2+}$ , filled circles are  $\text{O}^-$ , and open circles are  $\text{O}^{2-}$ . Each  $\text{O}^-$  forces its two neighboring Cu spins to be parallel to each other. (a) shows that an isolated  $\text{O}^-$  can cause three pairs of Cu spins in the linear  $\text{Cu}-\text{O}^{2-}-\text{Cu}$  chain to be parallel, thus creating three "frustrated" bonds. In (b) a pairing of two  $\text{O}^-$  produces a net of only two frustrated bonds, which may serve as a candidate for the bosonic field  $\phi$ . (c) and (d) show clusterings of four  $\text{O}^-$  and six  $\text{O}^-$ ; these configurations do not produce any frustrated bonds of Cu spins. (c) and (d) may provide nonlinear attractive interactions for  $\phi$ .

reduction factor due to polarization and screening.) Figure 2(c) suggests that the coefficients of  $\rho^2$  in  $u(\rho)$  may be negative, which can be the origin of the attractive interaction. From Fig. 2(c), one sees that it is not possible to cram six  $\text{O}^-$  into a unit lattice square; this makes the coefficient  $\rho^3$  in  $u(\rho)$  positive. [Figure 2(d) may lead to an additional, but nonlocal, small attractive  $\rho^3$  interaction.] Because of stability due to Coulomb repulsion at very close distances,  $u(\rho) \rightarrow \infty$  as  $\rho \rightarrow \infty$ . In Figs. 2(c) or 2(d), since the gain in  $\epsilon_{\uparrow\downarrow}$  is approximately a few  $\times 10^{-1}$  eV, after its cancellation with the Coulomb energy, the net gain might be approximately  $\times 10^{-2}$  eV, which determines the gap energy  $\Delta$ , and is consistent with a  $T_c \sim 10^2$  K.

### E. Extraplanar oxygen

It is generally agreed that superconductivity takes place in the  $\text{CuO}_2$  planes which are the one feature common to all the high- $T_c$  ceramics. Since these planes have always the same structure, it seems difficult to account for the marked difference in  $T_c$  among La 2:1:4, Y 1:2:3, etc. Although the proximity of two such planes in Y 1:2:3 may lead (as we shall show) to concentration of charge on one layer, that would still not make Y 1:2:3 far more favorable

to superconductivity than La 2:1:4, if the function  $u(\rho)$  within a layer were the same for both.

We are therefore led to compare the immediate neighborhoods of  $\text{CuO}_2$  layers in different ceramics. In La 2:1:4, the neighboring plane on each side contains an  $\text{O}^{2-}$  corresponding to each  $\text{Cu}^{2+}$  site in the superconducting layer, so that the  $\text{Cu}^{2+}$  is really surrounded not by four but by six oxygen sites forming an octahedron. But in Y 1:2:3, only one neighboring plane provides an  $\text{O}^{2-}$  so that each  $\text{Cu}^{2+}$  is surrounded by only five oxygen atoms making a square pyramid. The diagonal of the square base is  $\sim 3.8 \text{ \AA}$ , while the height of the pyramid (i.e., the half-length of the octahedron) is only  $\sim 2.4 \text{ \AA}$ . It seems natural then to speculate that the extraplanar oxygen neighbors weaken the pairing mechanism in the plane so as to account for the higher  $T_c$  in Y 1:2:3 (which has only one such extraplanar oxygen) than in La 2:1:4 (which has two). This appears reasonable since we are interested only in a small change of energy  $\approx 10^{-2} \text{ eV}$ . The idea draws support, if the pairing mechanism depends on the frustration of antiferromagnetism, from the fact that Néel temperatures are also about twice as high in Y 1:2:3 as in La 2:1:4 compounds.

In the  $n > 2$  compounds, the outer two layers are "pyramidal" while the inner one(s) are "planar"—the  $\text{Cu}^{2+}$  ions have only four oxygen neighbors. Let  $u_{\text{oct}}(\rho)$ ,  $u_{\text{pyr}}(\rho)$ , and  $u_{\text{pl}}(\rho)$  be, respectively, the local energy density function  $u(\rho)$  when the  $\text{Cu}^{2+}\text{O}_2^-$  square in Fig. 2(c) is the midplane of an octahedron (as in La 2:1:4), is the square base of a single pyramid (as in Y 1:2:3), and is on an isolated  $\text{CuO}_2$  plane (the middle plane in Tl 2:2:2:3 or Bi 2:2:2:3). We expect the minimum of these three functions, labeled by  $-\Delta_{\text{oct}}$ ,  $-\Delta_{\text{pyr}}$ , and  $-\Delta_{\text{pl}}$ , to satisfy the inequality

$$\Delta_{\text{oct}} < \Delta_{\text{pyr}} < \Delta_{\text{pl}}. \quad (1.16)$$

Schematic drawings of these three  $u(\rho)$  are given in Fig. 3. As will also be speculated on in Sec. III, the critical temperature  $T_c$  for  $n=1, 2$ , and 3 reflects the different values  $\Delta_{\text{oct}}$ ,  $\Delta_{\text{pyr}}$ , and  $\Delta_{\text{pl}}$ , which makes  $T_c$  rise with increasing  $n$  for  $n \leq 3$ . However,  $T_c$  for  $n=4$  may turn out to be less than  $T_c$  for  $n=3$ .

High-temperature superconductivity is a rapidly growing field. Yet, its underlying mechanism is still not understood. Many of the model-dependent statements made in

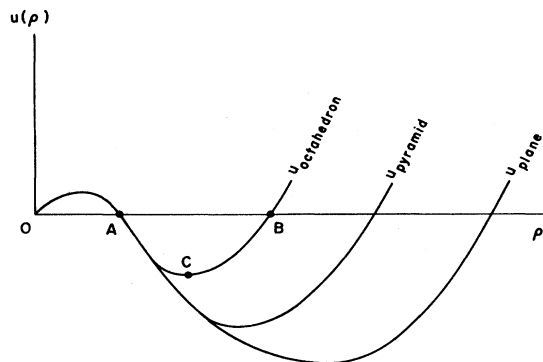


FIG. 3. Schematic drawings of  $u(\rho)$  when the  $\text{Cu}^{2+}\text{O}_2^-$  square in Fig. 2(c) is the midplane of an octahedron (as in La 2:1:4), is the square base of a single pyramid (as in Y 1:2:3), and is on an isolated  $\text{CuO}_2$  plane (as the middle plane in Tl 2:2:2:3).

this paper are conjecture. Nevertheless, since the long-range Coulomb force is known exactly and is not sensitive to the model at small distances, an examination of its role should be of some value.

## II. CHARGED SQUARE-LATTICE LAYERS

In order to evaluate the long-range Coulomb energy (1.10), it is useful to have on hand the solutions to the following problems in electrostatics.

### A. A single plane of charged square lattice

Consider first a two-dimensional square lattice that lies on the  $z=0$  plane in a Cartesian three-dimensional space. The lattice sites are located at

$$\mathbf{r}_n = \hat{\mathbf{e}}_x n_1 d + \hat{\mathbf{e}}_y n_2 d, \quad (2.1)$$

where  $\hat{\mathbf{e}}_x$  and  $\hat{\mathbf{e}}_y$  are unit vectors parallel to the  $x$  and  $y$  axes,  $d$  is the lattice spacing, and  $n_1$  and  $n_2$  are integers. On each site we place a charge of the same value  $q$ . To avoid the technical difficulty of the long-range  $r^{-1}$  Coulomb potential, we introduce the Yukawa potential  $V(\mathbf{r})$  at a point outside the lattice ( $\mathbf{r} \neq \mathbf{r}_n$ ):

$$V(\mathbf{r}) = q \int_{-\infty}^{\infty} dx' \int_{-\infty}^{\infty} dy' \sum_{n_1=-\infty}^{\infty} \sum_{n_2=-\infty}^{\infty} \delta(x' - n_1 d) \delta(y' - n_2 d) \frac{e^{-\mu R}}{R}, \quad (2.2)$$

where  $\mu$  is a small positive parameter ( $\mu \rightarrow 0$  in the end),

$$R = |\mathbf{r}' - \mathbf{r}| \quad (2.3)$$

with

$$\mathbf{r} = (x, y, z) \text{ and } \mathbf{r}' = (x', y', 0). \quad (2.4)$$

When  $\mathbf{r}$  coincides with the lattice point, say  $\mathbf{r}=0$ , define  $V_0$  to be the Yukawa potential due to all other charges:

$$V_0 \equiv q \sum_{\mathbf{r}_n \neq 0} e^{-\mu r_n} / r_n \quad (2.5)$$

where  $r_n = |\mathbf{r}_n|$ , and the sum extends over all lattice sites  $\mathbf{r}_n \neq 0$ .

Next, replace the discrete charge distribution by a uniform surface charge density

$$\sigma = q/d^2 \quad (2.6)$$

on the same  $z=0$  plane. The corresponding Yukawa potential is

$$\bar{V}(\mathbf{r}) = \sigma \int_{-\infty}^{\infty} dx' \int_{-\infty}^{\infty} dy' \frac{e^{-\mu R}}{R}. \quad (2.7)$$

In the limit  $\mu=0$ ,  $V$  and  $\bar{V}$  become the Coulomb potentials; both are divergent but the difference is finite. Define

$$v(\mathbf{r}) \equiv \lim_{\mu \rightarrow 0} [V(\mathbf{r}) - \bar{V}(\mathbf{r})] \quad (2.8)$$

and

$$v_0 \equiv \lim_{\mu \rightarrow 0} [V_0 - \bar{V}(0)]. \quad (2.9)$$

It will be shown in Appendix B that

$$v_0 = \frac{q}{d} \left[ -\frac{4\pi}{3} + \kappa \right], \quad (2.10)$$

where

$$\kappa = \sum'_m \left[ \frac{3\pi}{\sinh^2(\pi m)} - \frac{e^{-\pi m}}{m \sinh(\pi m)} \right] = 0.2885 \quad (2.11)$$

and, for  $z \neq 0$ ,  $v(\mathbf{r})$  is

$$v(x, y, z) = q \sum'_m (md)^{-1} \exp[2\pi(im_1x + im_2y - m|z|)/d] \quad (2.12)$$

with  $m = (m_1^2 + m_2^2)^{1/2}$  and the sum  $\sum'_m$  extends over all integral values of  $m_1, m_2$  except  $m_1 = m_2 = 0$  (these notations will be used throughout the paper).

In the following, we shall frequently encounter the value of  $v(\mathbf{r})$  at two particular positions,  $\mathbf{r} = (0, 0, z)$  and  $\mathbf{r} = (\frac{1}{2}d, \frac{1}{2}d, z)$  with  $z \neq 0$ :

$$v(0, 0, z) = q \sum'_m (md)^{-1} e^{-2\pi m|z|/d} \quad (2.13)$$

and

$$v(\frac{1}{2}d, \frac{1}{2}d, z) = q \sum'_m (md)^{-1} (-1)^{m_1+m_2} e^{-2\pi m|z|/d}. \quad (2.14)$$

The difference between the Coulomb energy per unit area of the above discrete and uniform charge distributions is

$$\frac{1}{2} \frac{qv_0}{d^2} = \frac{1}{2} \frac{q^2}{d^3} \left[ -\frac{4\pi}{3} + \kappa \right] = -1.9501 \sigma^2 d, \quad (2.15)$$

which, as expected,  $\rightarrow 0$  as  $d \rightarrow 0$  (at a fixed-surface charge density  $\sigma$ ).

#### B. $N=2$ tetragonal lattice with alternate layers of opposite charges

Define an " $N=2$ " tetragonal lattice to be one whose unit cell consists of two parallel layers of  $d \times d$  square lattice, placed at a distance  $c_1$  or  $c_2$  from each other so that from the lattice site of one layer we can reach that of the other by a displacement of  $c_1$  or  $c_2$ , perpendicular to the layer (analogous to the two  $\text{CuO}_2$  planes in  $\text{Y 1:2:3}$ ). The volume per cell  $(c_1 + c_2)d^2$ . As illustrated in Fig. 4(a), different lattice sites on the same layer carry identical charges,  $+q$  or  $-q$ , with the sign switching back and forth from layer to layer. We call those with  $+q$  "even layers," and those with  $-q$  "odd layers."

Next, define a modified  $N=2$  tetragonal lattice by

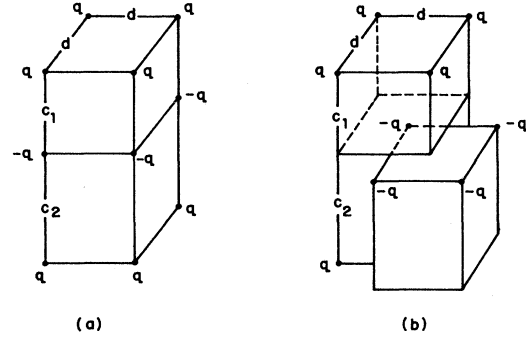


FIG. 4. Examples of (a) the unit cell of an  $N=2$  tetragonal lattice and (b) that of a modified  $N=2$  tetragonal lattice.

starting from an  $N=2$  tetragonal lattice, keeping its even layers fixed, but moving all odd lattice sites parallel to the squares along the diagonal direction, changing from corners to centers (of the original squares), as illustrated in Fig. 4(b).

The Coulomb energy of the entire lattice is given by

$$2\mathcal{N}u_c \equiv \frac{1}{2} \sum_{i \neq j} q_i q_j / r_{ij}, \quad (2.16)$$

where  $\mathcal{N}$  is the total number of unit  $d \times d \times (c_1 + c_2)$  cells,  $i$  and  $j$  run separately over all lattice sites (with  $i \neq j$ ), and  $q_i = q$  or  $-q$  depending on whether  $i$  is on the even or odd layers. Thus,  $2u_c$  is the Coulomb energy per unit cell, and  $u_c$  is that per unit square of each layer. By using (2.8)–(2.14), we derive

$$u_c = \frac{q^2}{2d} \left[ 2\pi \left( \frac{c_1 c_2}{(c_1 + c_2)d} - \frac{2}{3} \right) + \kappa + \sum'_m w_m \right], \quad (2.17)$$

where  $\kappa$  is given by (2.11) and

$$w_m = \frac{1}{m} (1 - e^{-2\pi m c/d})^{-1} [2e^{-2\pi m c/d} - (\pm 1)^{m_1+m_2} \times (e^{-2\pi m c_1/d} + e^{-2\pi m c_2/d})], \quad (2.18)$$

in which the upper sign is for the  $N=2$  tetragonal lattice, the lower sign for the modified one, and

$$c = c_1 + c_2. \quad (2.19)$$

In (2.17), the first term in the square brackets gives a contribution

$$\bar{u}_c = \frac{q^2 \pi c_1 c_2}{(c_1 + c_2)d^2} \quad (2.20)$$

to  $u_c$ . This is the Coulomb energy if the discrete charges are replaced by alternate layers of uniform surface charge densities  $+\sigma$  and  $-\sigma$ , where  $\sigma = q/d^2$ . The Coulomb energy  $\bar{u}_c$  for the continuum is always positive; its minimum is when  $\sigma=0$ . If we identify  $\pm q$  as the charge fluctuation, this means that the continuum energy  $\bar{u}_c$  is always against charge fluctuations between layers.

In the discrete case, when  $q=0$ ,  $u_c$  is 0. However, depending on the ratios  $c_1/d$  and  $c_2/d$ ,  $u_c$  may be  $< 0$ , in

which case the Coulomb interaction would favor charge fluctuations between even and odd layers. For example, when  $c_1 = c_2 = d$ , according to (2.17) and (2.18)  $u_c$  is negative. This may appear strange, since the electric forces are attractive between charges on neighboring layers but repulsive between charges on the same layer; the former holds only in one direction, say along the  $z$ -axis perpendicular to the layer, while the latter holds in two directions, along both  $x$  and  $y$ . Note that for any given charge, among its six nearest neighbors, two are attractive and four are repulsive, giving a net positive Coulomb energy. On the other hand, among its twelve next nearest neighbors, eight are attractive and only four repulsive, which gives a net negative Coulomb energy, etc. The total Coulomb energy summing over all charges is (2.17), which converges rapidly and is negative in this example.

### C. $N$ -layer tetragonal lattice

Generalize the problem to a tetragonal lattice whose unit cell now contains  $N$  layers of  $d \times d$  squares, as illustrated in Fig. 5(a) for  $N=4$ . The volume per unit cell is

$$d \times d \times [(N-1)c_1 + c_2], \quad (2.21)$$

where  $c_1$  is the spacing between nearest-neighboring layers in the same cell, and  $c_2 > c_1$ . Label these layers consecutively by

$$v=1, 2, \dots, N. \quad (2.22)$$

Different lattice sites on the same layer carry the same charge  $q_v$ , with

$$\sum_1^N q_v = 0 \quad (2.23)$$

so that  $q_v$  represents charge fluctuation. Our problem is to find the minimum of Coulomb energy keeping *fixed* the

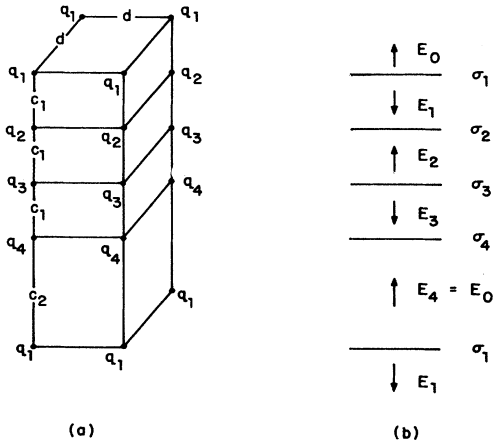


FIG. 5. (a) The unit cell for an  $N=4$  tetragonal lattice. (b) Distributions of surface charges  $\sigma_v$  and the electric fields between surfaces.

total charge fluctuation

$$Nq^2 \equiv \sum_1^N q_v^2. \quad (2.24)$$

The solution can be derived in two steps.

(i) Consider a related problem in which each layer of discrete charges is replaced by a uniform charge density

$$\sigma_v = q_v/d^2. \quad (2.25)$$

Correspondingly, let the  $z$ -component electric field between the  $v$ th and the  $(v+1)$ th layers be

$$E_z \equiv (-1)^v E_v, \quad (2.26)$$

where the  $z$  axis is perpendicular to the layers. Hence,

$$\begin{aligned} E_0 + E_1 &= 4\pi\sigma_1, & E_1 + E_2 &= -4\pi\sigma_2, \dots, \\ E_{N-1} + E_N &= (-1)^{N-1} 4\pi\sigma_N \end{aligned} \quad (2.27)$$

with  $E_0$  as the electric field along the  $z$  direction above the first layer, as shown in Fig. 5(b). From (2.27), we have

$$4\pi \sum_1^N \sigma_v = E_0 - (-1)^N E_N. \quad (2.28)$$

Hence, (2.23) gives the boundary condition for each cell:

$$E_0 = (-1)^N E_N. \quad (2.29)$$

The Coulomb energy per unit cell for the continuum case is

$$N\bar{u}_c \equiv \frac{d^2}{8\pi} \left[ c_1 \sum_1^{N-1} E_v^2 + c_2 E_N^2 \right]. \quad (2.30)$$

The constraint (2.24) becomes

$$\sum_1^N \sigma_v^2 \equiv N\sigma^2 = N(q/d^2)^2 \quad (2.31)$$

being kept fixed. The minimum of  $\bar{u}_c$  can be obtained by setting, when  $N$  is *odd*,

$$\begin{aligned} E_0 = E_N &= 0, \\ E_v &= 4\pi\sigma \left[ 1 + \cos\left(\frac{\pi}{N}\right) \right]^{-1/2} \sin\left(\frac{v\pi}{N}\right), \end{aligned} \quad (2.32)$$

$$\sigma_v = (-1)^{v+1} \sigma \sqrt{2} \sin\left[\frac{v-(1/2)\pi}{N}\right].$$

The corresponding Coulomb energy per unit  $d \times d$  square per layer is, on account of (2.31),

$$\bar{u}_c = \frac{\pi q^2 c_1}{[1 + \cos(\pi/N)] d^2}. \quad (2.33)$$

When  $N$  is *even*, the minimum  $\bar{u}_c$  configuration is

$$E_v = 4\pi\sigma \left[ \frac{\tan(\theta/2)}{\sin\theta + N^{-1} \sin(N\theta)} \right]^{1/2} \cos[(\frac{1}{2}N - v)\theta], \quad (2.34)$$

$$\begin{aligned} \sigma_v &= (-1)^{v+1} \sigma \left[ \frac{2 \sin\theta}{\sin\theta + N^{-1} \sin(N\theta)} \right]^{1/2} \\ &\times \cos\left[ \left( \frac{N+1}{2} - v \right) \theta \right], \end{aligned}$$

where  $\theta$  is an angle between 0 and  $\pi/N$ , determined by

$$\tan\left(\frac{1}{2}\theta\right)\tan\left(\frac{1}{2}N\theta\right) = (c_2/c_1) - 1. \quad (2.35)$$

The corresponding minimum Coulomb energy (per unit  $d \times d$  square per layer) is

$$\bar{u}_c = \frac{\pi q^2 c_1}{(1 + \cos\theta)d^2}. \quad (2.36)$$

In these solutions,  $\sum_1^N \sigma_\nu = 0$  by construction. From (2.32) and (2.33), we see that

$$\sigma_\nu = (-1)^{N+1} \sigma_{N+1-\nu}. \quad (2.37)$$

Therefore, for  $N$  even, the sum of all odd powers of  $\sigma_\nu$  is zero:

$$\sum_1^N \sigma_\nu^3 = \sum_1^N \sigma_\nu^5 = \dots = 0. \quad (2.38)$$

For  $N$  odd, these sums are not all zero; e.g., by using

$$w_m = \frac{1}{m} (1 - e^{-2\pi mc/d})^{-1} \left[ 2e^{-2\pi mc/d} + \frac{1}{N} \sum_{\nu \neq \nu'} (q_\nu q_{\nu'} / q^2) \{ \exp(-2\pi m | \nu' - \nu | c_1 / d) + \exp[-2\pi m (c - | \nu' - \nu | c_1) / d] \} \right], \quad (2.42)$$

and  $c = (N-1)c_1 + c_2$ .

The following remarks should be noted.

(i) When  $N$  is odd, we may combine two neighboring  $d \times d \times c$  tetragons (that share a common  $d \times d$  square) to be the new unit cell. Label the squares consecutively by [instead of (2.22)]

$$\nu = 1, \dots, N, N+1, \dots, 2N, \quad (2.43)$$

and replace the constraint (2.23) by

$$\sum_1^{2N} q_\nu = 0. \quad (2.44)$$

One can readily verify that the minimum  $\bar{u}_c$  for the continuum case is now given by the same expression (2.36), which was valid previously only for  $N$  even. Correspondingly,  $E_\nu$  and  $\sigma_\nu$  are given by (2.34), with  $\nu$  now running from 1 to  $2N$ . We see that (for  $N$  odd), in contrast to (2.29),  $E_0 + E_N \neq 0$ , but

$$E_0 - E_{2N} = 4\pi \sum_1^{2N} \sigma_\nu = 0, \quad (2.45)$$

where, as before,  $\sigma_\nu = q_\nu / d^2$ . Because  $\theta$  in (2.35) is  $< \pi/N$ , this new  $\bar{u}_c$  given by (2.36) is smaller than that given previously by (2.33).

(ii) For applications, we are interested in the energy difference between  $q_\nu = 0$  (no charge fluctuation) and  $q_\nu \neq 0$  (charge fluctuation between neighboring  $\text{CuO}_2$  planes). Both configurations have the same average charge density. At zero temperature, the system is assumed to be entirely in the Bose-liquid phase. As remarked before, the absence of the Fermi gas (normal conduction electron) makes it unnecessary to examine its

(2.32) we find

$$\sum_1^N \sigma_\nu^3 = 0 \text{ if } N \neq 3. \quad (2.39)$$

When  $N=3$ ,

$$\sigma_1 : \sigma_2 : \sigma_3 = -1 : 2 : -1; \quad (2.40)$$

this gives  $\sum_1^N \sigma_\nu^3 = 3\sigma^3 / \sqrt{2}$ . Thus, for problems in which the energy is sensitive to the cubic power of charge fluctuations, the  $N=3$  case may play a special role.

When  $c_2 \rightarrow \infty$ , the angle  $\theta$  in (2.35) becomes  $\pi/N$ ; hence, (2.34) and (2.36) (for  $N$  even) become (2.32) and (2.33) (for  $N$  odd).

(ii) Return to the discrete case. We set  $q_\nu = \sigma_\nu d^2$  as determined by the continuum solution. By using (2.10)–(2.13), we find the Coulomb energy per unit square per layer to be

$$u_c = \bar{u}_c + \frac{q^2}{2d} \left[ -\frac{4\pi}{3} + \kappa + \sum'_m w_m \right], \quad (2.41)$$

where  $\bar{u}_c$  is given by (2.33) or (2.36),  $\kappa = 0.2885$ ,

screening effect. However, in order to take into account the polarization of other material present, we divide the energies (2.16), (2.17), and (2.41) by a dielectric constant  $\epsilon$ .

### III. APPLICATIONS

#### A. La 2:1:4 ( $n=1$ )

Although La 2:1:4 belongs to the  $n=1$  family where  $n$  is the number of  $\text{CuO}_2$  layers per cell, actually its geometry is more similar to the modified  $N=2$  tetragonal lattice discussed in Sec. IIB but with "tetragonal" replaced by "orthorhombic." For the application of (2.17) and (2.18), set

$$c_1 = c_2 = 6.5916 \text{ \AA} \quad (3.1)$$

and (as a lower bound)

$$d = \frac{1}{2}(a+b) = 3.7725 \text{ \AA}. \quad (3.2)$$

By using the lower sign in (2.18), we find the long-range Coulomb energy per  $\text{CuO}_2$  square due to charge fluctuations to be

$$u_c = 0.7944 \times q^2 / \epsilon d > 0, \quad (3.3)$$

which shows that the long-range Coulomb force is against charge fluctuation between neighboring  $\text{CuO}_2$  planes.

To justify the use of (2.17) and (2.18), let  $Q_i$  be the charge-density operator of the  $\phi$  field at the  $i$ th lattice site, as in (1.10). Define  $\langle Q_i \rangle$  to be its expectation value

$$Q \equiv N^{-1} \sum_i \langle Q_i \rangle \quad (3.4)$$



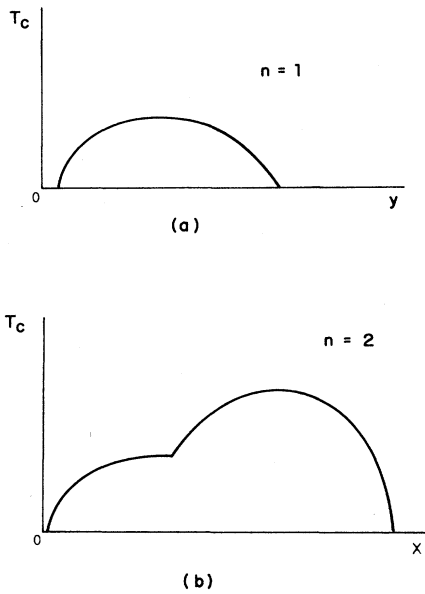


FIG. 6. (a) For  $(\text{La}_{1-y}\text{Sr}_y)_2\text{CuO}_4$  ( $n=1$ ), the absence of charge fluctuations makes  $T_c$  vs the doping parameter  $y$  a smooth function. (b) For  $\text{YBa}_2\text{Cu}_3\text{O}_{6.5+x}$  ( $n=2$ ),  $T_c$  vs the doping parameter  $x$  has a "steplike" shape because of charge fluctuations between neighboring  $\text{CuO}_2$  planes.

and

$$q_i \equiv \langle Q_i \rangle - Q, \quad (3.5)$$

where  $\mathcal{N}$  is the total number of lattice sites. Consider a fluctuation distribution in which the average of  $q_i$  is  $+q$  on any even  $\text{CuO}_2$  layer and  $-q$  on any odd  $\text{CuO}_2$  layer; otherwise, assume (i)  $q_i$  distributes randomly. In addition, as mentioned before, the constraint  $i \neq j$  in (1.10) is equivalent to assuming (ii)  $d=a$  or  $b$ , which becomes (3.2) since  $a \cong b$ .

From (1.10), (3.4), and (3.5), it follows that  $U_c$  is a quadratic function of  $q$ . The linear term vanishes because of the symmetry in interchanging the even and odd layers. By using assumptions (i) and (ii), one sees that  $U_c$  can be written as

$$U_c = U_c(\rho) + u_c \quad (3.6)$$

where  $u_c$  is given by (3.3) and  $U_c(\rho)$  is the long-range Coulomb energy when the boson density  $\rho$  is a uniform one. The minimum of (1.6) is  $q=0$  and  $U = \Omega \langle u(\rho) \rangle$  where the total energy density is

$$\langle u(\rho) \rangle = u(\rho) + \Omega^{-1} U_c(\rho). \quad (3.7)$$

Schematically  $\langle u(\rho) \rangle$  for  $\text{La } 2:1:4$  has the same form as  $u_{\text{oct}}$  in Fig. 3. Superconductivity occurs only along the segment  $ACB$  on the curve, when  $\langle u(\rho) \rangle$  is  $< 0$  and therefore the Bose liquid is stable. Since  $kT_c$  is approximately  $-\langle u(\rho) \rangle$  and  $\rho=y$  in accordance with (1.15), the typical variation of  $T_c$  vs  $y$  for  $n=1$  is a smooth one, illustrated in

Fig. 6(a). (At very small value of  $y \leq 0.025$ , before superconductivity sets in,  $\text{La } 2:1:4$  has a complicated phase diagram,<sup>8</sup> which lies outside the simple Fermi-gas model discussed here.)

### B. Y 1:2:3 ( $n=2$ )

For Y 1:2:3, we use the upper sign in (2.18). Set as in (3.2)

$$d = \frac{1}{2}(a+b) = 3.863 \text{ \AA}, \quad (3.8)$$

$$c_1 = 3.332 \text{ \AA} \text{ and } c_2 = 8.334 \text{ \AA}. \quad (3.9)$$

Equation (2.17) gives

$$u_c = -0.02388 \times q^2 / \epsilon d < 0. \quad (3.10)$$

Hence, the long-range Coulomb forces have a slight preference for charge fluctuations between neighboring  $\text{CuO}_2$  planes.

Define  $\langle u(\rho) \rangle$  to be the total energy density when the boson density  $\rho$  is uniform, as in (3.7). For Y 1:2:3, it has the same form as  $u_{\text{pyr}}$  in Fig. 3. Because of charge fluctuation, the actual energy density is given by

$$v(\rho) = \frac{1}{2} [\langle u(\rho + \sigma) \rangle + \langle u(\rho - \sigma) \rangle], \quad (3.11)$$

which is not a smooth function of  $\rho$ . For  $\rho$  not too small, we may take the simple example of  $\langle u(\rho) \rangle = -b\rho^2 + c\rho^3$  with both  $b$  and  $c$  positive. The minimum of (3.11) is given by a fluctuating boson density

$$\sigma = \begin{cases} \rho & \text{if } \rho < \rho_I, \\ 0 & \text{if } \rho > \rho_I, \end{cases} \quad (3.12)$$

where  $\rho_I = b/3c$  is the point inflection of  $\langle u(\rho) \rangle$ , and that gives

$$v(\rho) = \begin{cases} 2c\rho^2(2\rho - 3\rho_I) & \text{if } \rho < \rho_I, \\ c\rho^2(\rho - 3\rho_I) & \text{if } \rho > \rho_I. \end{cases} \quad (3.13)$$

Setting  $kT_c \sim -v(\rho)$  and  $\rho = \frac{1}{2}x$  in accordance with (1.15), the typical variation of  $T_c$  versus the doping parameter  $x$  for the  $n=2$  family is illustrated in Fig. 6(b), consistent with experimental result.<sup>17</sup>

### C. Tl 2:2:2:3 ( $n=3$ )

For Tl 2:2:2:3, the Coulomb energy  $u_c$  per unit square per  $\text{CuO}_2$  layer due to charge fluctuation is given by a modified version of (2.41) with  $N=3$ :

$$u_c = \frac{q^2}{2\epsilon d} \left[ \frac{4\pi}{3} \left( \frac{c_1}{d} - 1 \right) + \kappa + \sum'_m w_m \right] \quad (3.14)$$

where  $\kappa = 0.2885$ ,  $q^2$  is determined by (2.24),  $w_m$  is given by [instead of (2.42)]

$$\begin{aligned}
w_m = & (2/3m)(1 - e^{-4\pi mc/d})^{-1} \{ 3e^{-4\pi mc/d} - 2(e^{-2\pi mc/d} + e^{-2\pi m(2c-c_1)/d}) \\
& + \frac{1}{2}(e^{-4\pi mc_1/d} + e^{-4\pi m(c_1+c_2)/d}) - 3(-1)^{m_1+m_2} e^{-2\pi mc/d} \\
& + (-1)^{m_1+m_2} [2(e^{-2\pi m(3c_1+c_2)/d} + e^{-2\pi m(c_1+c_2)/d}) - \frac{1}{2}(e^{-2\pi mc_2/d} + e^{-2\pi m(2c-c_2)/d})] \},
\end{aligned} \tag{3.15}$$

and  $c = 2c_1 + c_2$ . Setting  $d = \frac{1}{2}(a+b) = 3.8503 \text{ \AA}$ ,  $c_1 = 3.2 \text{ \AA}$ , and  $c_2 = 11.54 \text{ \AA}$ , we have

$$u_c = -0.2251 \times q^2 / \epsilon d \tag{3.16}$$

which is in favor of charge fluctuation, with the fluctuating charge distribution on the three CuO<sub>2</sub> layers given by (2.40).

In addition, the internal energy  $u(\rho)$  is  $u_{pl}$  for the mid-CuO<sub>2</sub> layer, which is expected to be lower than  $u_{pyr}$  for the two outer layers. Thus,  $u(\rho)$  and  $u_c$  together like to concentrate as many superconducting carriers as possible into the midlayer. Because of (1.16), we expect the maximum  $T_c$  for different  $n$  to satisfy

$$T_c(n=1) < T_c(n=2) < T_c(n=3). \tag{3.17}$$

In contrast, for  $n=4$ , the optimal fluctuating charge distribution is, according to (2.34) and (2.35) for  $c_2 \gg c_1$ ,

$$\sigma_1 : \sigma_2 : \sigma_3 : \sigma_4 = -1 : \sqrt{2} + 1 : -\sqrt{2} - 1 : 1. \tag{3.18}$$

Hence, it is not possible to concentrate all the superconducting carriers in the two midplanes (i.e., the second and third layers), and that suggests

$$T_c(n=2) < T_c(n=4) < T_c(n=3). \tag{3.19}$$

#### ACKNOWLEDGMENTS

We wish to thank Y. Uemura, M. K. Wu, and M. Kastner for helpful discussions. This research was supported in part by the U.S. Department of Energy.

#### APPENDIX A

In the Bose-liquid and Fermi-gas model, each individual boson by itself, is unstable:

$$\phi \rightarrow 2 \text{ holes}. \tag{A1}$$

In accordance with (1.4) and (1.5), the mass difference is  $< \Delta$ , approximately a few  $\times 10^{-2}$  eV. As the temperature rises from zero, the gas systems form a two-dimensional Fermi sea of holes. (The average spacing between CuO<sub>2</sub> planes is quite wide,  $\sim 7 \text{ \AA} \gg a$  or  $b$ . Also, the effective mass in the direction perpendicular to the CuO<sub>2</sub> plane is expected to be much larger than the parallel direction; hence, as an approximation, we may neglect

the third dimension.) In each CuO<sub>2</sub> plane, the hole density  $n$  can be  $\sim \frac{1}{2}$  per unit lattice square (area  $a \times b$ ) for Y 1:2:3; the corresponding top Fermi kinetic energy  $k_F^2/2m_e$  is then  $\sim 0.7$  eV, as determined by ( $\hbar = 1$ )

$$n = k_F^2 / 2\pi. \tag{A2}$$

Because this energy is much greater than  $\Delta$ , a natural question is whether the Fermi sea would inhibit the evaporation of the Bose liquid. The following simple example illustrates why this may not be the case.

The average density of kinetic energy of the Fermi gas is

$$T = nk_F^2 / 4m_e. \tag{A3}$$

Between the fermions (holes), there must be a strong binary attractive potential to form the boson pair state. This gives for the Fermi-gas system an average potential-energy density  $V$  proportional to the pair density  $n^2$ . We may write

$$V = -(gn)^2 / m_e \tag{A4}$$

where  $g^2$  is  $O(1)$  and dimensionless. Hence

$$\frac{V}{T} = -\frac{2}{\pi} g^2 \tag{A5}$$

independent of  $k_F$ . For  $g^2 = \pi/2$ ,

$$V + T = 0 \tag{A6}$$

at any density of the Fermi gas. Therefore, once the boson becomes unstable at small  $k_F$ , the same holds at large  $k_F$ . The instability (A1) can then be viewed as the  $k_F = 0$  limit. This feature is true in two dimensions, or approximately in three dimensions if the Fermi surface is an ellipsoid of very large oblateness (as in the present problem).

The gap energy  $\Delta$  of the Bose liquid is due to an attractive  $\rho^2$  term in  $u(\rho)$ , introduced in (1.7). Translating to fermions, this means a nearly local attractive four-fermion interaction. Its effect on the Fermi gas may be neglected, since there is a reduction factor  $(nl^2)^2$ , where  $l$  is its range.

#### APPENDIX B

To establish (2.10)-(2.14), we follow the method developed by Madelung,<sup>18</sup> Benson,<sup>19</sup> and others.<sup>20</sup> Substitute

$$\sum_{n_2=-\infty}^{\infty} \sum_{n_1=-\infty}^{\infty} \delta(x - n_1 d) \delta(y - n_2 d) = d^{-2} \sum_{m_2=-\infty}^{\infty} \sum_{m_1=-\infty}^{\infty} \exp[i2\pi(m_1 x + m_2 y)/d] \tag{B1}$$

into (2.2), and derive for (2.8),  $\mathbf{r} = (0, 0, z)$ ,

$$v(0, 0, z) = \lim_{\mu \rightarrow 0} (q/d^2) \sum'_m h_m(z), \quad (\text{B2})$$

where the sum  $\sum'_m$  extends over all  $m_1, m_2$  except  $m_1 = m_2 = 0$ , and

$$h_m(z) \equiv \int dx dy r^{-1} \exp[-\mu r + 2\pi i(m_1 x + m_2 y)/d]. \quad (\text{B3})$$

Because  $\partial^2 h_m(z)/\partial z^2 = \kappa^2 h_m(z)$  with  $\kappa^2 = \mu^2 + (2\pi/d)^2 \times (m_1^2 + m_2^2)$ , we have  $h_m(z) = h_m(0) e^{-\kappa|z|}$ . It can be readily verified that as  $\mu \rightarrow 0$ ,  $h_m(0) = d/(m_1^2 + m_2^2)^{1/2}$ . Thus, we establish (2.13), and likewise also (2.12) and (2.14).

Next, consider the hypothetical problem of a simple cubic lattice of lattice spacing  $d$ , with a charge  $q$  on each lattice site. The Yukawa potential at  $\mathbf{r} = 0$  is

$$Y_0 \equiv q \sum'_n e^{-\mu r_n / r_n}, \quad (\text{B4})$$

where  $r_n = (n_1^2 + n_2^2 + n_3^2)^{1/2} d$  and the sum  $\sum'_n$  extends over all integral  $n_1, n_2$ , and  $n_3$ , except  $n_1 = n_2 = n_3 = 0$ . At any given  $n_3$ , replace the discrete planar charge distribution by a uniform surface charge density  $q/d^2$ ; the corresponding Yukawa potential at  $\mathbf{r} = 0$  is

$$\bar{Y}(0) = \sum_{n_3=-\infty}^{\infty} (q/d^2) \int dx dy e^{-\mu r / r}, \quad (\text{B5})$$

where  $r = (x^2 + y^2 + z^2)^{1/2}$  and  $z = n_3 d$ . Carrying out the integration and the summation, we have

$$\bar{Y}(0) = 2\pi q \left[ \mu d^2 \tanh \frac{\mu d}{2} \right]^{-1}. \quad (\text{B6})$$

Define, similar to  $v_0$  in (2.9),

$$y_0 \equiv \lim_{\mu \rightarrow 0} [Y_0 - \bar{Y}(0)]. \quad (\text{B7})$$

By using (2.13), we see that

$$y_0 - v_0 = 2q \sum'_m (md)^{-1} (e^{2\pi m} - 1)^{-1}, \quad (\text{B8})$$

where, as in (2.12),  $m = (m_1^2 + m_2^2)^{1/2}$  and  $\sum'_m$  sums over all integral  $m_1$  and  $m_2$ , except  $m_1 = m_2 = 0$ . On the other hand,  $Y_0$  is also given by

$$Y_0 = qd^2 \sum'_n r_n^{-3} (n_1^2 + n_2^2 + n_3^2) e^{-\mu r_n} \\ = 6q \sum_{n_3=1}^{\infty} (z/d)^2 g(z), \quad (\text{B9})$$

where  $z = n_3 d$  as before, and  $g(z) = d^2 \sum_{n_1, n_2} r_n^{-3} e^{-\mu r_n}$  which, on account of (B1), can be written as

$$g(z) = g_0(z) + \sum'_m g_m(z), \quad (\text{B10})$$

with

$$g_0(z) = \int dx dy r^{-3} e^{-\mu r}, \quad (\text{B11})$$

$$g_m(z) = \int dx dy r^{-3} \exp[-\mu r + 2\pi i(m_1 x + m_2 y)/d], \quad (\text{B12})$$

and  $r = (x^2 + y^2 + z^2)^{1/2}$ . Letting  $\hat{\mathbf{r}} = \mathbf{r}/z$ , we have  $g_0(z) = (2\pi/z) \int \hat{\mathbf{r}}^{-2} e^{-\mu z \hat{\mathbf{r}}} d\hat{\mathbf{r}}$  and therefore

$$\sum_{n_3=1}^{\infty} n_3^2 g_0(n_3 d) = 2\pi \mu \int_{\mu d}^{\infty} \frac{e^{-u}}{u^2 (1 - e^{-u})^2} du. \quad (\text{B13})$$

Furthermore, at  $\mu = 0$ ,  $g_m(z) = (2\pi/z) e^{-2\pi m z/d}$ . This plus (B6) and (B13) give, for (B7),

$$y_0 = (4\pi q/d) \left[ -\frac{1}{3} + 3 \sum'_n e^{-2\pi n} (1 - e^{-2\pi n})^{-2} \right] \quad (\text{B14})$$

on account of

$$-\frac{4\pi}{3} = \lim_{\mu \rightarrow 0} \pi \left[ 3\mu d \int_{\mu d}^{\infty} \frac{du}{u^2 \sinh^2(\frac{1}{2} u)} - \frac{2}{\mu d \tanh(\frac{1}{2} \mu d)} \right]. \quad (\text{B15})$$

Combining (B8) with (B14), we prove (2.10).

<sup>1</sup>P. Chaudhari *et al.*, Phys. Rev. B **36**, 8903 (1987).

<sup>2</sup>T. K. Worthington, W. J. Gallagher, and T. R. Dinger, Phys. Rev. Lett. **59**, 1160 (1987).

<sup>3</sup>Z. Schlesinger *et al.*, Phys. Rev. B **35**, 5334 (1987).

<sup>4</sup>F. London, *Superfluids* (Wiley, New York, 1954).

<sup>5</sup>Compare M. R. Schafroth, Phys. Rev. **96**, 1442 (1954); M. R. Schafroth and J. M. Blatt, *ibid.* **100**, 1221 (1955). Their treatment is based on a gapless Bose-Einstein transition of the Bose-gas system. Their model differs from ours in almost all the major features.

<sup>6</sup>R. Friedberg and T. D. Lee, Mod. Phys. Lett. B **2**, 469 (1988).

<sup>7</sup>T. D. Lee, Nature **330**, 460 (1987); in *Two-dimensional Strongly Correlated Electronic Systems* (Gordon and

Breach, New York, in press); Mod. Phys. Lett. B **3**, 135 (1989).

<sup>8</sup>A. Aharony *et al.*, Phys. Rev. Lett. **60**, 1330 (1988).

<sup>9</sup>R. J. Birgeneau, M. A. Kastner, and A. Aharony, Z. Phys. B **71**, 57 (1988).

<sup>10</sup>Y. Uemura (private communication).

<sup>11</sup>J. C. Bednorz and K. A. Müller, Z. Phys. B **64**, 189 (1986).

<sup>12</sup>T. Fujita *et al.*, Jpn. J. Appl. Phys. **26**, L368 (1987).

<sup>13</sup>M. K. Wu, J. R. Ashburn, C. J. Torng, P. H. Hor, R. L. Meng, L. Gao, Z. J. Huang, Y. Q. Wang, and C. W. Chu, Phys. Rev. Lett. **58**, 908 (1987).

<sup>14</sup>Z. X. Zhao *et al.*, Kexue Tongbao **6**, 412 (1987).

<sup>15</sup>*Proceedings of the Adriatico Research Conference on High-*

- Temperature Superconductors*, edited by S. Lundqvist, E. Tosatti, M. Tosi, and Yu Lu (World Scientific, Singapore, 1987), *Proceedings of the Beijing International Workshop on High-Temperature Superconductivity*, edited by Z. Z. Gan, G. J. Cui, G. Z. Yang, and Q. S. Yang (World Scientific, Singapore, 1987).
- <sup>16</sup>P. W. Anderson, *Phys. Rev.* **115**, 2 (1959).
- <sup>17</sup>R. Cava, in *Proceedings of the Adriatico Research Conference on High Temperature Superconductivity* (World Scientific, Singapore, 1987), p. 167.
- <sup>18</sup>E. Madelung, *Z. Phys.* **19**, 524 (1918).
- <sup>19</sup>G. C. Benson, *Can. J. Phys.* **34**, 888 (1956).
- <sup>20</sup>M. L. Glasser and I. J. Zucker, *Theoretical Chemistry, Advances and Perspectives* (Academic, New York, 1980), pp. 67–139.